Toxicology Reports 2 (2015) 111–120

Contents lists available at ScienceDirect

Toxicology Reports

journal homepage: www.elsevier.com/locate/toxrep

# One time nose-only inhalation of MWCNTs: Exploring the mechanism of toxicity by intermittent sacrifice in Wistar rats

Arul Prakash Francis[a], Selvam Ganapathy[b], Venkata Rajsekhar Palla[b], Prakhya Balakrishna Murthy[b], Sundara Ramaprabhu[c], Thiyagarajan Devasena[a,*]

[a] Centre for Nanoscience and Technology, A.C. Tech Campus, Anna University, India
[b] International Institute of Biotechnology and Toxicology (IIBAT), Padappai, India
[c] Alternative Energy and Nanotechnology Laboratory (AENL), Nanofunctional Materials Technology Centre (NFMTC), Department of Physics, Indian Institute of Technology Madras, Chennai, India

ARTICLE INFO

*Article history:*
Received 18 November 2014
Received in revised form 8 January 2015
Accepted 1 February 2015
Available online 7 February 2015

*Keywords:*
MWCNT
Inhalation
Toxicity
Fibrosis
Cytokines
Intermittent

ABSTRACT

We have investigated the time-dependent effect of multi-walled carbon nanotubes (MWCNTs) in rats upon single inhalation exposure followed by intermittent sacrifice. The effects were monitored by analyzing the bronchoalveolar lavage fluid (BALF) and histopathological analysis. Cell count, neutrophils, lymphocytes, lactate dehydrogenase, alkaline phosphatase, protein and cytokines (tumor necrosis factor-alpha (TNF-α) and interleukin 4 (IL-4)) were significantly increased, while cell viability and alveolar macrophage count significantly decreased in the BALF of MWCNT-treated rats on day 1, day 7 and day 14 post-exposure, when compared to control rats. Histopathological analysis revealed inflammation, fibrosis and granuloma in the lungs of MWCNTs-treated rats on day 7 and day 14 post-exposure. We interpret that MWCNT induces inflammation, fibrosis and granuloma characterized by progressive elevation of TNF-α and IL-4. Histopathological studies further support our view and reveal the distribution of MWCNT in lungs and tracheobronchial lymph nodes (TBLN). We conclude that MWCNT-induced pulmonary toxicity is considerable even on single exposure.


## 1. Introduction

Carbon nanotubes (CNTs) due to their unique properties are making a breakthrough in industries and biomedicine [1]. As a result, the production rate of CNTs is rising considerably. Recent reports reveal that the global production of CNTs exceeds several thousand tons per year [2]. In this scenario, the exposure of the environment including human beings and the ecosystem to CNTs and the threat of CNT toxicity are also increasing. However, the information about the possible human health and environmental impacts produced by CNTs is still scanty. CNTs exhibit a toxic potential, similar to those observed with fibrous materials due to their high aspect ratio [3]. CNTs induced dose-dependent severity of the lesions like persistent epitheloid granulomas and interstitial inflammation in mice after single intra-tracheal treatment was observed [4]. In mice and rats, pulmonary inflammation characterized by alterations in cellularity and enzyme activities of bronchoalveolar lavage fluid (BALF) and microscopic findings like infiltration of macrophage, granulomas, and fibrosis were observed after intra-tracheal administration of SWCNTs or MWCNTs [5–7]. Long MWCNTs with needle shaped structure, similar

* Corresponding author at: Centre for Nanoscience and Technology, Anna University, Chennai 600 025, India. Tel.: +91 9962645151.
*E-mail addresses:* fdapharma@gmail.com (A.P. Francis), sebhu.edu@gmail.com (S. Ganapathy), vrspalla@gmail.com (V.R. Palla), prakhya@yahoo.com (P.B. Murthy), ramp@iitm.ac.in (S. Ramaprabhu), tdevasenabio@annauniv.edu, tdevasenabio@gmail.com (T. Devasena).

http://dx.doi.org/10.1016/j.toxrep.2015.02.003

to asbestos, produce asbestos-like pathological changes after intraperitoneal injection [8]. Moreover, histopathological lesions were observed in the in the upper and lower parts of respiratory tract after inhalation exposure of rats to MWCNTs. Previous studies reported the inflammatory changes by examining the BALF, which revealed the variation in polymorphonuclear neutrophils, macrophages, lymphocytes and expression of inflammatory cytokines [9,10]. However, the time dependent studies on effects of CNTs in lung after one time nose-only inhalation and the mechanism of toxicity are limited.

We investigated the time dependent pulmonary toxicity of MWCNTs after one time nose-only inhalation of MWCNTs followed by intermittent sacrifice on day 1, 7 and 14 post-exposure in rat model. The concentrations of MWCNTs were selected based on permissible exposure limit of carbon materials such as graphite as reported by National Institute for Occupational Safety and Health, USA [34]. The inflammatory and fibrotic responses in the lung of MWCNTs-inhaled rats were examined by the changes in the lung histopathology, alveolar macrophages, neutrophils, lymphocytes and the expression of TNF-α and IL-4 in the broncho-alveolar lavage fluid.

## 2. Experimental details

### 2.1. Materials

MWCNTs (purity > 95%), obtained as gift sample from Department of Physics, IIT, Madras, were used for the current study. Cytokine kits (Tumor Necrosis Factor-alpha (TNF-α) and Interleukin-4 (IL-4)) were purchased from Ray Biotech USA. All other chemicals and reagents used for the study were procured from Sigma–Aldrich Corporation, India.

### 2.2. Animals

Twenty-four male Wistar rats with body weight 180–200 g, free from clinical signs of disease, were obtained from the Animal house, International Institute of Biotechnology and Toxicology (IIBAT), Padappai, India. The protocol of animal study was approved by Institutional Animal Ethics Committee (6/106/IAEC/2013). The rats were divided into four groups and housed in polypropylene cages in a room on a 12:12-h light/dark photoperiod at a temperature of 23 ± 2 °C and relative humidity of 53 ± 5%. Rats were provided with gamma-irradiated rodent pellet feed (Tetragon Chemie Pvt. Ltd., Bangalore, India) and reverse osmosis water *ad libitum* except during the exposure period. Animals were permitted to acclimatize to the animal room conditions for one week before the initiation of the study. All animals were acclimatized for 6 h to the inhalation system on 2 consecutive days before start of the exposure period and the experimental conditions were similar to those used in pilot study.

### 2.3. Characterization of MWCNTs

The structural alignment of MWCNTs and purity were determined from X-ray diffraction analysis using Rigaku diffract meter with Cu-Kα radiation λ = 1.54060 Å. The diffraction pattern was obtained in the range of $2\theta = 20–80^{\circ}$. The obtained diffraction pattern was compared with standard JCPDS values to determine their crystal system and its related parameter. Moreover, the surface morphology of MWCNTs was determined using high-resolution scanning electron microscope HRSEM (FEI Quanta FEG 200, Japan) and FEI Tencai 30 G2 S-TWIN high-resolution transmission electron microscopy (HRTEM). The elemental analysis (EDAX) was done by RTEM2 EDAX, AMETEK operating at 250 kV.

### 2.4. MWCNTs exposure

Male Wistar rats were exposed to MWCNTs using nose-only inhalation exposure chambers (CH. Technologies, USA) for 4 h, to an aerosol concentration of 5 mg/m$^3$. The concentrations of MWCNTs were selected based on permissible exposure limit of carbon materials such as graphite as reported by National Institute for Occupational Safety and Health (NIOSH) [34]. The inhalation systems contain three major modules: an aerosol generator – Wright Dust Feeder (BGI, Inc.), a rodent nose-only inhalation exposure chamber and an aerosol concentration measurement device – gravimetric single filter (BGI, Inc.). The rats were kept in glass restraint tubes (attached to the wall of the cylinder) with their snouts projecting into the inhalation chamber. The dilution of the aerosol in the breathing zone with external air was avoided by generating positive pressure inside the inhalation chamber. Moreover, the whole exposure system was kept under exhaust hoods in an air-conditioned room. MWCNTs aerosols were generated using the Wright Dust feeder, which was connected to the inlets of each inhalation chamber. The actual concentrations of the MWCNTs in the inhalation chambers were determined gravimetrically 3 times during each exposure day. In addition, samples were taken twice from the exposure chambers to determine the mass median aerodynamic diameter (MMAD) and geometric standard deviation (GSD) using a Mercer seven-stage cascade impactor (CH Technologies, USA). A pilot study was performed in advance to the animal exposure by generating MWCNT aerosols continuously for 4 h in inhalation chamber to realize the particle size distribution of the generated aerosol.

To explore the exacerbation of toxic effects of MWCNTs exposure due to the biopersistance of nanotubes, the rats were sacrificed on day 1, day 7 and day 14 post-exposure. The toxicity potential was determined by observing body weight, food consumption parameters, and the clinical signs of toxicity throughout the study.

### 2.5. Broncho-alveolar lavage fluid analysis

Rats were euthanized with an overdose of Thiopentone I.P. (Thiosol$^{TM}$ sodium) via intraperitoneal injection. The right portion of the lungs of rats was immediately lavaged twice with 5 mL of $Ca^{2+}$, $Mg^{2+}$ free phosphate buffered saline (Himedia, India). About 90% of the total volume instilled was retrieved and the volume is similar in all groups. The lavage collections were centrifuged

at 400 × *g* for 10 min at 4 °C. The cell pellet obtained was re-suspended in RPMI 1640 (Himedia, India) and used for the estimation of cell viability as well as total and differential cell counts. Cell viability was determined using trypan blue dye and the total cells were counted in an Automatic Cell Counter (Countess™ automated cell counter, Invitrogen). Differential cell counts were done using the slides prepared by cytocentrifuge, which was fixed using methanol and stained with Geimsa stain. A total of 500 cells per slide were counted randomly from 10 different sites under an oil-immersion microscope with 1000× magnification for alveolar macrophages, neutrophils and lymphocytes, which were identified by their characteristic cell morphology. The biochemical parameters (lactate dehydrogenase (LDH), alkaline phosphatase (ALP) and total protein (TP)) and cytokines analysis were performed using the supernatant. Biochemical assays were done spectrophotometrically using a Dimension Xpand plus (Siemens, USA) clinical chemistry analyser.

### 2.6. Cytokine estimation

Pro-inflammatory cytokine, i.e., tumor necrosis factor-alpha (TNF-α) (Ray Biotech, USA) and pro-fibrotic cytokine i.e., interleukin-4 (IL-4), levels were quantified in bronchoalveolar lavage fluid (BALF) using ELISA kits according to the manufacturer's instructions. The amount of cytokine was estimated using the standard curve obtained from cytokine standards included in the kits.

### 2.7. Histopathology

The left portion of the lung along with the tracheobronchial lymph nodes from all animals was collected and preserved in 10% neutral-buffered formalin. The lungs were inflated with 10% neutral-buffered formalin before preservation. The organs were processed in a vacuum infiltration tissue processor (Sakura Tissue-Tek® VIP™, Japan), embedded (Sakura Tissue-Tele TEC™, Japan) in paraffin wax, sectioned (Microm GmbH, Germany) at approximately 5 μm thick, stained (Leica ST5020-Autostainer, Germany) with hematoxylin and eosin, viewed under light microscope (Nikon50i, Japan), and the images were captured through an image analyser (Q-Imaging systems, Canada). The identity and analysis of the pathology slides were blind to the pathologist.

### 2.8. Statistical analysis

Statistical analyses were conducted with SAS 9.3 software. Data were expressed as mean ± SD ($n = 6$). Data from different time points were compared using a one-way analysis of variance followed by Student–Newman–Keuls Test. A criterion for statistical significance for all tests was set at $P < 0.05$ and levels of significance were represented for each result.

## 3. Results and discussion

The size and the morphology of MWCNTs were determined using HRSEM and HRTEM while the composition and the purity were determined using EDAX and XRD. The X-ray diffraction pattern of the MWCNTs is shown in Fig. 1. The diffraction peak in the XRD pattern of MWCNTs clearly confirms the removal of catalytic impurities. The lower alignment of MWCNTs was explained by the strong (0 0 2) peak in the XRD pattern. The HRSEM and HRTEM images of MWCNTs are shown in Fig. 2. The surface morphology of MWCNTs is clearly revealed in both the images (size scale 100 nm). The diameter of MWCNTs was found to be 15–50 nm. The micrographs also clearly indicate the dimensions and packing density of MWCNTs showing the partial alignment of MWCNTs. The EDAX result showed a major peak of carbon that confirmed the purity as shown in Fig. 3.

We determined the magnitude of inhalation toxicity of MWCNTs by intermittent sacrifice at days 1, 7 and 14 post-exposure in male Wistar rats. BALF parameters and lung histopathology were used as toxicity indices.

The animals were exposed to MWCNTs followed by a pilot study, which explains the particle size distribution of the generated aerosol. The particle size distribution is an

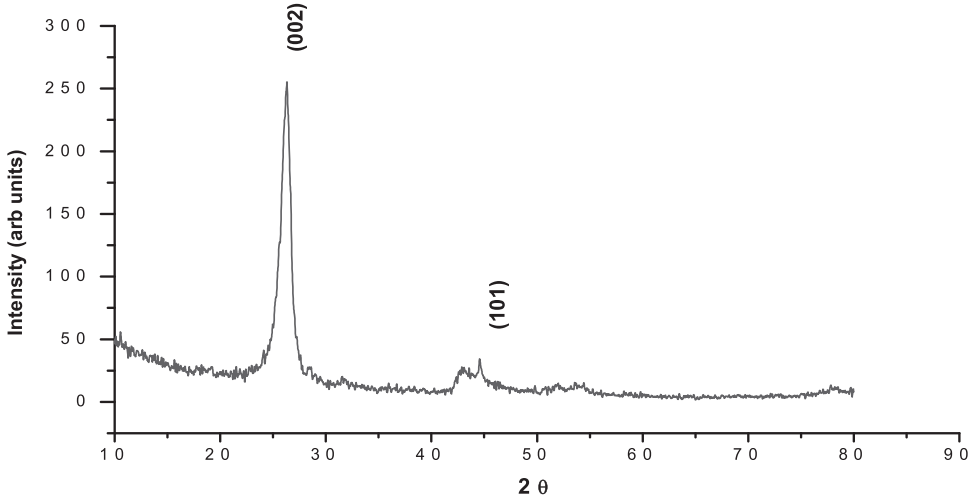


**Fig. 1.** X-ray diffraction pattern of MWCNTs.

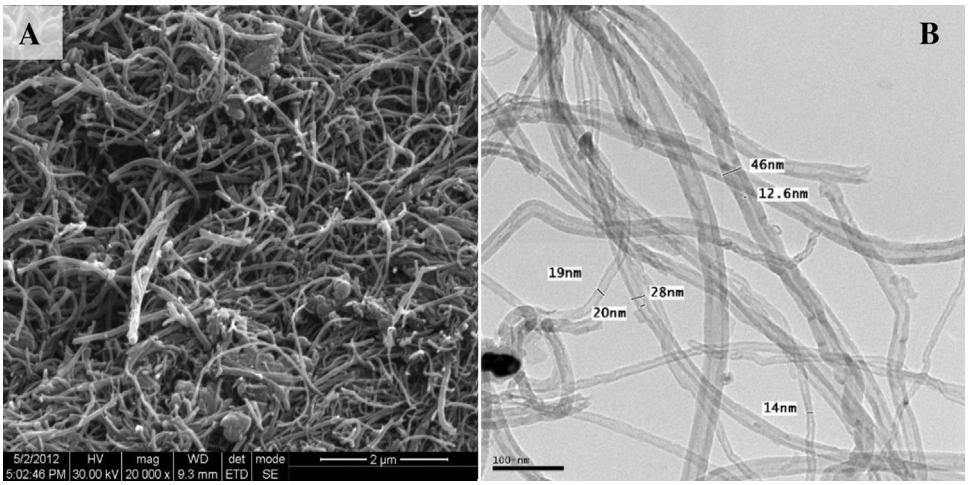


**Fig. 2.** (A) HRSEM and (B) HRTEM images showing the surface morphology of MWCNTs.

essential parameter that explains tendency of the deposition of nanomaterials in lung. A previous study reported by Ryman-Rasmussen et al. [11], Myojo et al. [12] and Geraets et al. [13] reveals the size dependent deposition of particles in the respiratory tract. The rats were exposed to MWCNTs for of 4 h continuously at an average actual aerosol concentration of 5 mg/m$^3$, while the control rats were exposed to clean air. The distribution of aerosol particles was assessed periodically and found to have an average MMAD of 1.82 μm and average GSD of 2.54 μm. The temperature and relative humidity at the breathing zone were determined at proper interval of time and found to be 21–22.30 °C and 50–55% respectively. Oxygen concentration was above 21% all through the experiment. All these parameters confirm that the aerosols were not static.

### 3.1. Cytological and biochemical analysis of BALF

Cell count and the cell viability of the BALF sample are shown in Fig. 4. Single inhalation exposure of MWCNTs resulted in a significant increase in the cell count in day 1 when compared to control. The cell count attained a peak at day 7 and was significantly higher than the control and the day 1 sample. This increase could be due to (i) recruitment of macrophages, neutrophils and lymphocytes upon inflammation and (ii) rupture of alveolar epithelium results in the release of epithelial cells induced by MWCNTs [9]. A slight decrease in cell count (but not significant) was observed in day 14 compared to the rats sacrificed at day 7 which may due to the fall in the free MWCNTs in the alveolar space owing to phagocytosis.

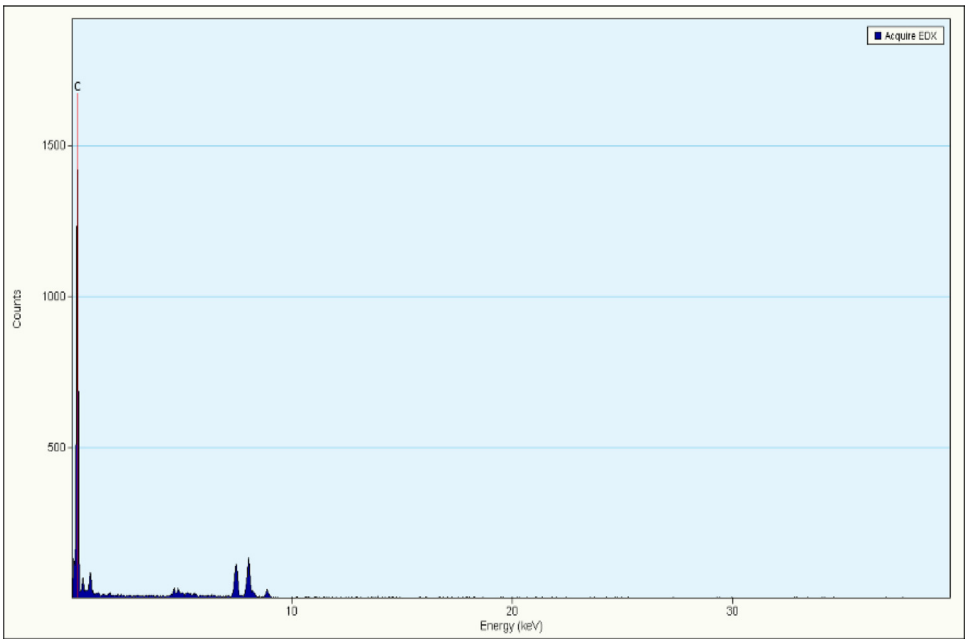


**Fig. 3.** EDAX profile with dominant peaks of Carbon.

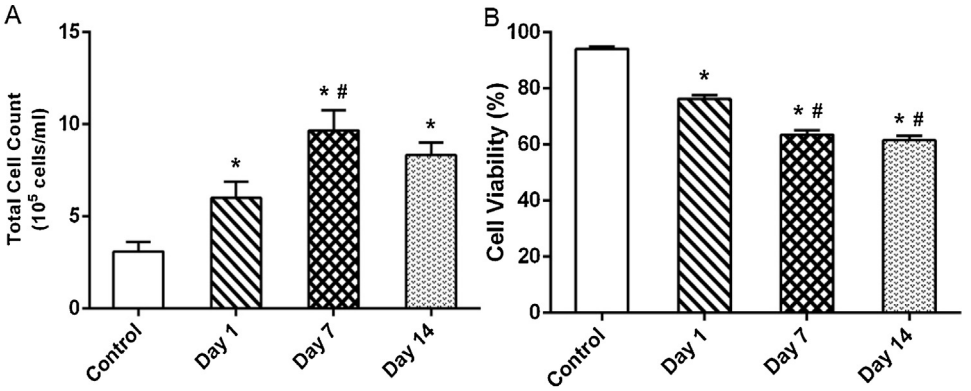


**Fig. 4.** Changes in the (A) total cell count (quantified using cell counter) and (B) cell viability in BALF collected from the rats exposed to MWCNTs for 4 h and sacrificed intermittently on different days (days 1, 7 and 14) after inhalation. Values are expressed in mean ± S.D.; ($n = 6$ animals/group). *Values are statistically significant from the control group ($P < 0.05$). #Values are significantly different from MWCNTs exposed rats sacrificed on day 1 post-exposure ($P < 0.05$).

A significant decrease in the viability of BALF cells was observed at all the three time points compared with that of control rats (Fig. 4). The fall in cell viability was results from (i) Cellular oxidative stress in the lungs and (ii) Mechanical damage in the alveolar epithelium induced by MWCNTs. Moreover the nanoparticles with fibrous and oblong morphology such as CNTs could be produce macrophage cell damage during their engulfment. This may also result in loss of cell viability The current findings were coincides with the previous studies reported by Ma-Hock et al. [9] and Srinivas et al. [14] on nanomaterials suggested that the significant increase in the total cell count and decrease in the cell viability of BALF was an indicator of pulmonary toxicity.

The respective percentage of BALF alveolar macrophages, neutrophil and lymphocyte counts are shown in Fig. 5. The presence of neutrophils and lymphocytes in BALF collected from animals sacrificed on 7th and 14th day after exposure is shown in Fig. 5B and C. The neutrophil count in BALF was found to be increased and reached a maximum of about 26% at day 7 post-exposure. As neutrophils are the characteristic indicators of initial stage of inflammation [15–17], we infer that inflammation is maximally reflected after a week of exposure to MWCNTs. The lymphocytes were marginally increased throughout the observation period with a peak at day 14 post-exposure. As lymphocyte elevation in the BALF is an index of chronic inflammatory response, we suggest that MWCNTs induces chronic inflammation. We hypothesize that the chronic inflammation may be due to biopersistence of MWCNTs in the lungs. This hypothesis is further supported by the histopathology of the lungs of the rats sacrificed on day 14 post-exposure (Fig. 9). The percentage of alveolar macrophages was found to be decreased in accordance with the relative increase of neutrophils and lymphocytes throughout the observation period (Fig. 5A).

Morphologically, MWCNT laden alveolar macrophages were noticed in rats sacrificed at day 1, day 7 and day 14 post-exposure. Binucleated and multinucleated alveolar macrophages of variable size possessing numerous cytoplasmic vacuoles were observed in the BALF of animals sacrificed on 7th and 14th day post-exposure (Fig. 6). Umeda et al. [18] reported that the presence of bi- and multi-nucleated macrophages was mainly due to the mitotic inhibition of alveolar macrophages with phagocytosed MWCNTs. We suggest that MWCNTs might have bound to the mitotic spindle thus preventing further division of macrophages.

Altered LDH and ALP activities together with total protein content in the lavage fluid are the markers of pulmonary disorders. We observed a significant and gradual increase in LDH, TP and ALP values increased gradually from day 1 to day 7 post-exposure (Fig. 7). However, on day 14 a slight decrease in all the parameters was observed when compared to day 7 after exposure. This may be due to a fall in the concentration of free MWCNTs in alveolar space.

MWCNTs induced cytotoxicity in the lung is confirmed by the significant leakage of protein and LDH from pulmonary epithelium. LDH concentration in BALF is measurable only in the presence of cell injury, while protein level in BALF was used as a marker to determine the integrity of the alveolar epithelial-capillary barrier. Our findings are in line with previous studies, which confirms the presence of LDH in BALF as an indication of the pulmonary damage [19–22]. The higher concentration of ALP point out the involvement of type II cells, which plays a major role in the repair of alveolar epithelium after injury. Previous reports also confirmed the increase of ALP activity (a marker of type II cell damage or proliferation) in BALF on exposure to pneumotoxicants [9,23–25].

### 3.2. Cytokine analysis of BALF

Fig. 8A and B shows the level of TNF-α and IL4 in the control and MWCNT-exposed rats. TNF-α content in the BALF of MWCNTs-exposed rats was significantly ($P < 0.05$) higher in day 1, day 7 and day 14 post-exposure. The degree of increase correlated directly with the days of post-exposure. The role of pro-inflammatory cytokines in the initiation and progression of inflammatory reaction was reported in various studies [26–29]. The increase in TNF-α in our study may

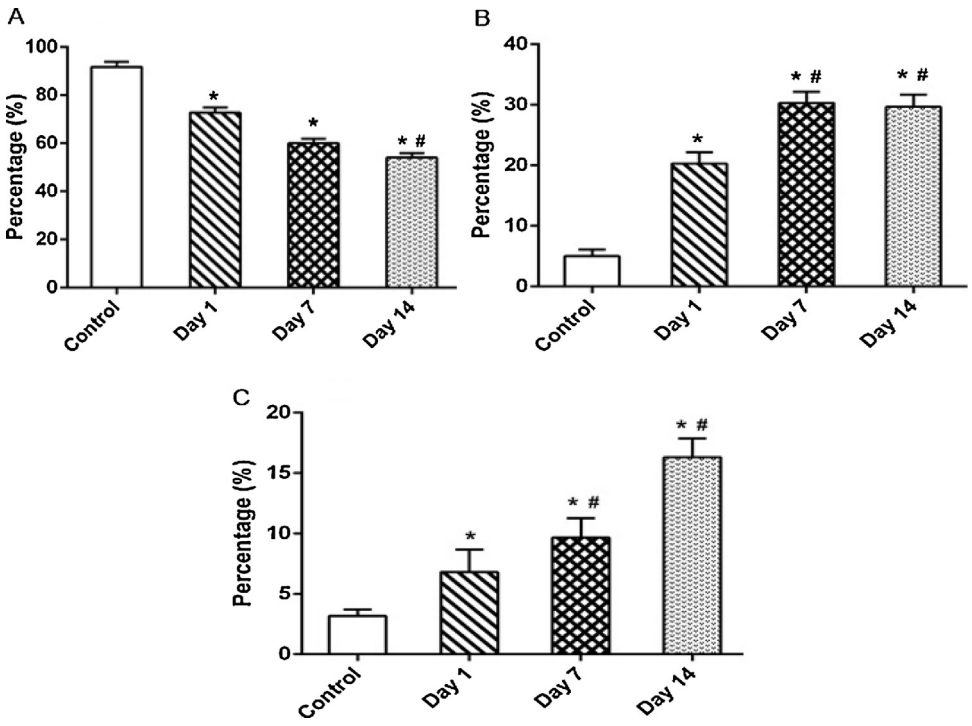


**Fig. 5.** Percentage of (A) alveolar macrophages, (B) neutrophils and (C) lymphocytes in BALF collected from the rats exposed to MWCNT for 4 h and sacrificed intermittently on day 1, 7 and 14 post-exposure. Values are expressed in mean ± S.D. ($n = 6$ animals/group). *Values are statistically significant from the control group ($P < 0.05$). #Values are significantly different from MWCNTs exposed rats sacrificed on day 1 post-exposure ($P < 0.05$).

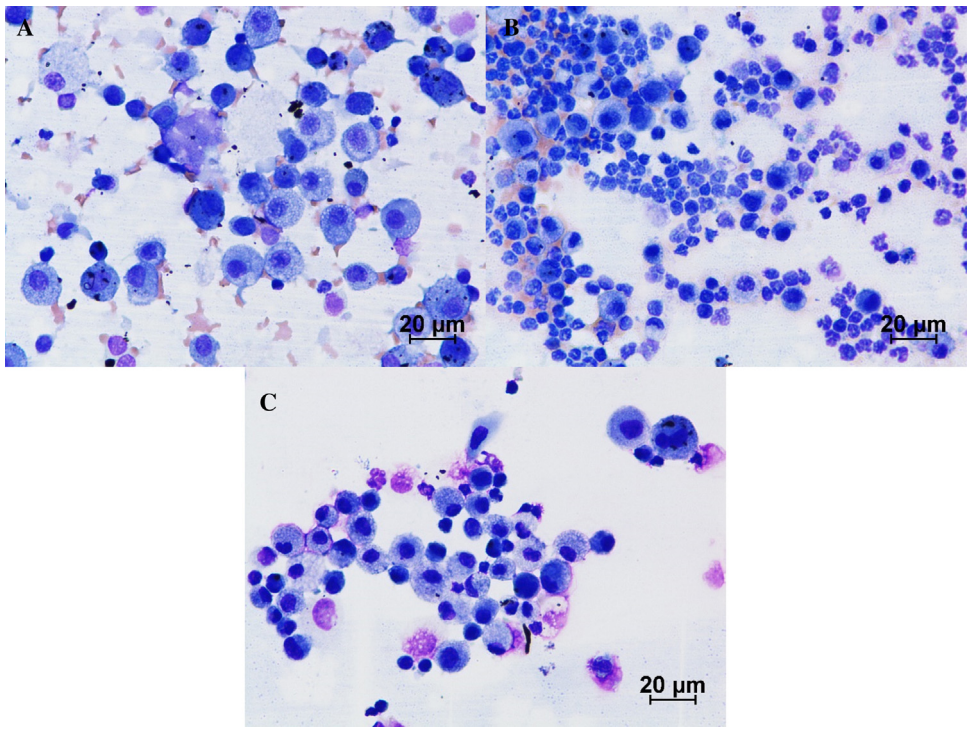


**Fig. 6.** Cytology of BALF on: (A) day 1 post-exposure, the cellularity of BALF was predominated with alveolar macrophages. Arrow indicates the MWCNT laden alveolar macrophages. (B) Day 7 post-exposure, the neutrophils were increased comparatively. (C) Day 14 post-exposure, tendency to increase in number of lymphocytes in BALF was observed. Giemsa ×400.

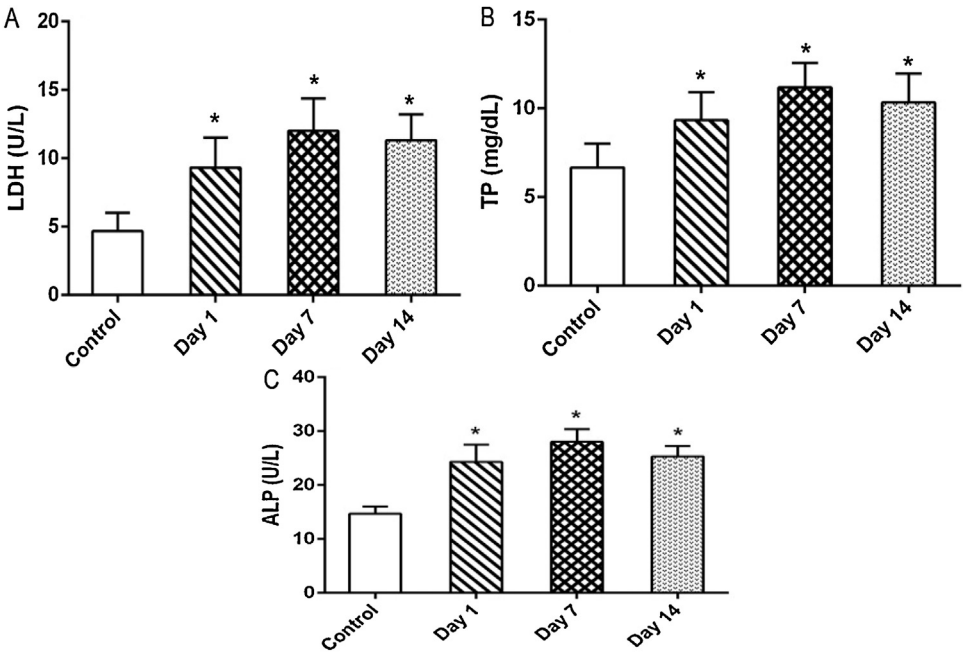


**Fig. 7.** The effect of MWCNTs on (A) LDH activity (B) TP content and (C) ALP activity in BALF collected from rats of rats exposed for 4 h and sacrificed intermittently on different days (days 1, 7 and 14) after inhalation. Values are expressed in mean ± S.D.; ($n$ = 6 animals/group). *Values are statistically significant from the control group ($P$ < 0.05).

be due to increase in inflammation and due to phagocytosis of MWCNT by macrophages.

IL-4 concentration in BALF of rats treated with MWCNTs did not show any differences on day 1 post-exposure compared to control groups. However level was significantly increased on day 7 and day 14 when compared to control rats. IL-4 is a profibrogenic cytokine [30]. Huaux et al. [31] have reported IL-4 as a reliable indicator of fibrosis in mice treated with bleomycin. Dose dependent fibrotic potential of intra tracheally instilled MWCNT in lung was previously reported by Muller et al. [32], by using an alternative fibrogenic index hydroxyl proline index. Correlating these reports with our findings we suggest that single exposure of MWCNTs upregulates IL-4 and induces pulmonary fibrosis. Our hypothesis can further be supported by the histopathological micrograph displayed in Fig. 9.

### 3.3. Histopathology studies

The histopathological changes observed in the lung and lung associated lymph nodes (tracheo-bronchial) of MWCNTs treated and the control animals are summarized in Table 1 and the microphotographs are illustrated in Fig. 9.

Microscopically, the MWCNT exposed lungs at all sacrifice time points have revealed the deposition of non-phagocytosed MWCNTs as black granular agglomerated masses in airways, alveolar lumen and interstitium (Fig. 9A–D). The alveolar macrophages with intracytoplasmic MWCNTs which is suggestive of phagocytosis were observed over bronchiolar epithelial lining (Fig. 9B), pulmonary interstitial space (Fig. 9A and C) and alveolar lumen (Fig. 9D) indicating rapid onset and continuum of pulmonary clearance mechanism. The appearance of

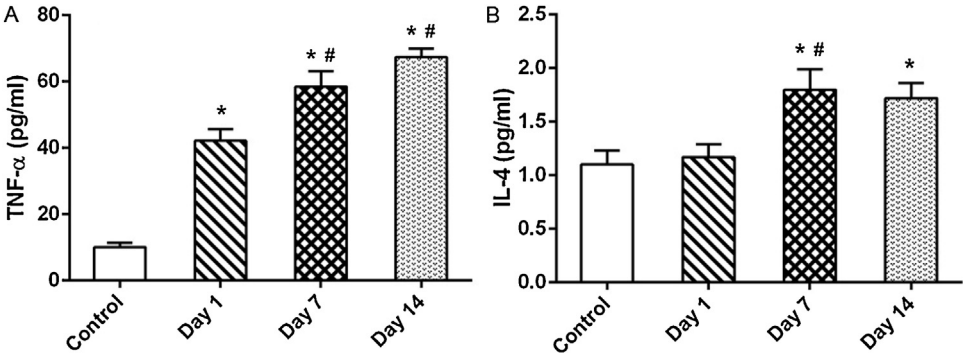


**Fig. 8.** Time-dependent changes in the concentration of (A) TNF-α and (B) IL-4 in BALF of rats exposed to MWCNTs for 4 h and sacrificed intermittently on different days (days 1, 7 and 14) after inhalation. Values are expressed in mean ± S.D.; ($n$ = 6 animals/group). *Values are statistically significant from the control group ($P$ < 0.05). #Values are significantly different from MWCNTs exposed rats sacrificed on day 1 post-exposure ($P$ < 0.05).

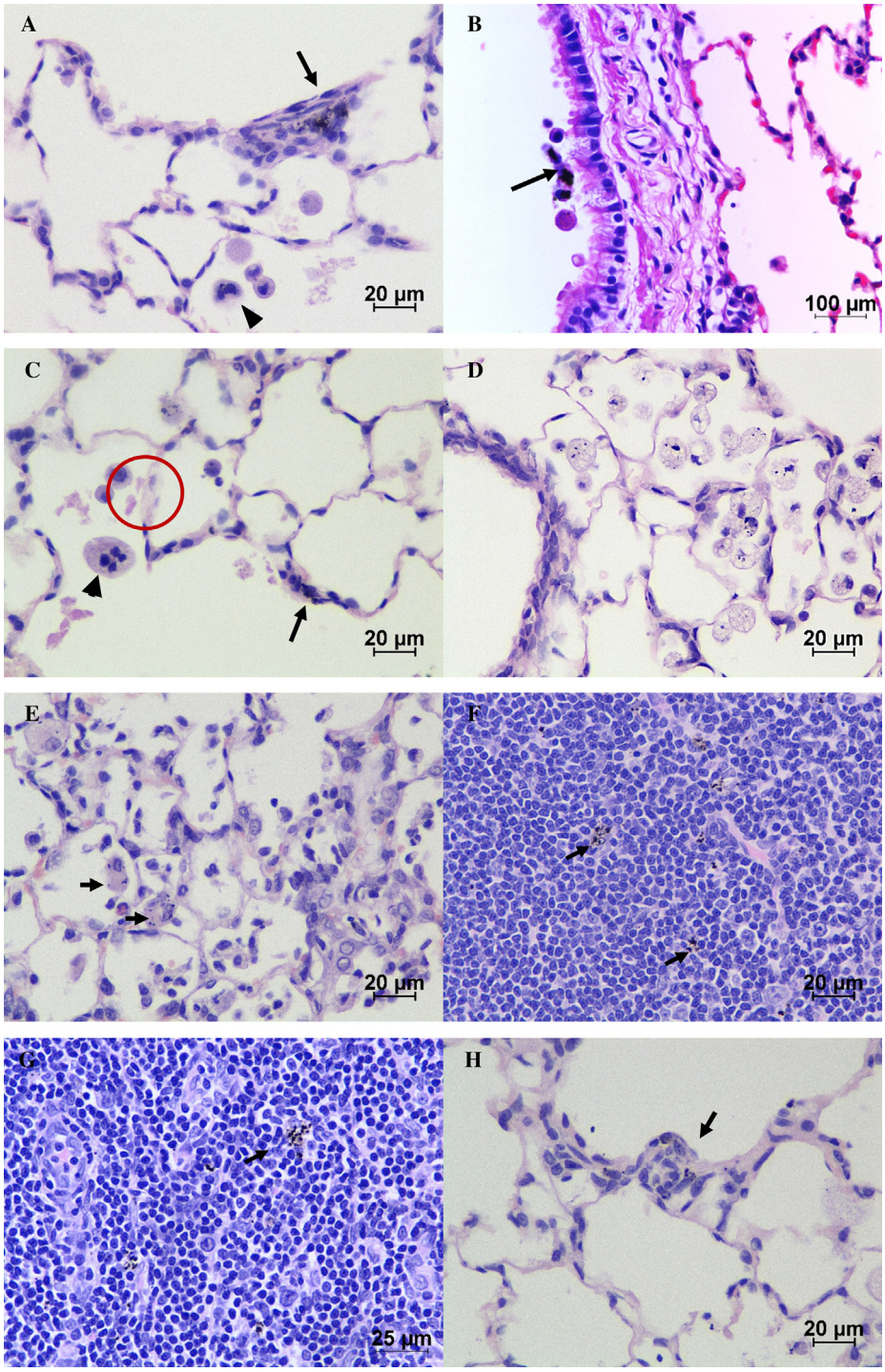


**Fig. 9.** Histopathological changes observed in the lungs and trachea-bronchial lymph nodes of MWCNT exposed rats. (A) Aggregates of MWCNT (arrow) in alveolar duct interstitium. Arrow head indicates the bi-nucleated alveolar macrophage. Note the alveolar wall thickening with proliferating interstitial fibroblasts. (B) Ciliary escalation of MWCNT laden macrophages (arrow) over bronchiolar epithelium (day 1 post-exposure). (C) Alveolar proteinosis with occasional multi-nucleated macrophages in alveolar lumen (arrow head). Arrow indicates the deposition of MWCNTs in alveolar interstitium. In addition the presence of granular, eosinophilic material (encircled) in the alveolar space (day 7 post-exposure). (D) Focal, moderate alveolar histiocytosis with prominent cytoplasmic vacuolation and phagocytosed MWCNT (day 7 post-exposure). (E) Chronic inflammation of alveoli. Arrow indicates the MWCNT laden histiocytes (day 14 post-exposure). (F and G) The presence of translocated MWCNT laden macrophages in trachea-bronchial lymph node at day 7 and day 14 post-inhalation respectively. (H) Focal to multifocal early stage epitheloid granuloma (arrow) at pulmonary interstitium (day 14 post-exposure). (H and E) ×400 (A, C–H), ×100 (B).

**Table 1**
Summary of histopathological lesions and pulmonary distribution of MWCNTs observed in the lungs of rat with MWCNTs for 4 h.

| Groups | Control | MWCNT | | |
|---|---|---|---|---|
| | | Day 1 | Day 7 | Day 14 |
| Total number of animals | 6 | 6 | 6 | 6 |
| No. of animals examined | 6 | 6 | 6 | 6 |
| Free MWCNTs, airways/alveoli | 0 | 6 | 6 | 3 |
| MWCNT laden macrophages, alveolar | 0 | 6 | 6 | 6 |
| MWCNT laden macrophages, BALT | 0 | 0 | 3 | 4 |
| MWCNT laden macrophages, TBLN | 0 | 0 | 4 | 6 |
| Histiocytosis, alveolar | 0 | 0 | 3 | 4 |
| Proteinosis, alveolar | 0 | 0 | 2 | 4 |
| Hyperplasia, lymphoid, BALT | 0 | 0 | 2 | 4 |
| Infiltrates, mononuclear, perivascular | 1 | 4 | 6 | 6 |
| Infiltrates, mixed, alveolar/interstitial | 1 | 0 | 3 | 6 |
| Inflammation, acute, alveolar | 1 | 3 | 3 | 0 |
| Inflammation, chronic, granulomatous[a], epitheloid, alveolar/interstitial | 0 | 0 | 4 | 6 |
| Fibrosis, interstitial | 0 | 0 | 4 | 5 |

BALT – bronchus associated lymphoid tissue; TBLN – tracheo-bronchial lymph node.
[a] Severity is based on the number and size of initial stage granulomatous lesion.

bi-, multi- and or anucleated alveolar macrophages with or without intracytoplasmic phagocytosed MWCNTs (Fig. 9A and C) was observed at all sacrifice time points.

Apart from the above microscopic findings, 3/6 animals showed acute pulmonary inflammation and 4/6 animals showed diffuse mononuclear inflammatory cell infiltration around pulmonary perivascular region on day 1 post-exposure. On day 7 post-exposure, the translocation of inhaled MWCNT was observed by the presence of MWCNT laden macrophages in BALT (intrapulmonary) and tracheo-bronchial lymph nodes (extrapulmonary) (Fig. 9F and G). The alveolar lumen had minimal to mild amount of granular, eosinophilic material (alveolar proteinosis) suggestive of ongoing pulmonary epithelial injury (Fig. 9A, C and H). Alveolar histiocytosis (Fig. 9D) characterized by the presence of two or more alveolar macrophages with enormous, highly vacuolated foamy cytoplasm in focal to multifocal areas of alveolar lumen were observed. Most of these macrophages had intracytoplasmic phagocytosed MWCNTs. Infiltration of mixed inflammatory cells in alveolar space along with acute pulmonary inflammation was observed. However, some animals showed the chronic inflammatory reactions with the development of early stage epitheloid granulomas (Fig. 9H) surrounding the MWCNTs and interstitial fibrosis along with acute inflammation on day 7 sacrifice time point. These granulomas were well organized, discrete, and multifocal and majorly distributed at centri-acinar regions. However, the appearance of either Langhan's giant cell or foreign body type giant cells was not found within the granulomas.

The histopathological changes confirm the biopersistence of MWCNTs, which leads to the chronic inflammation. Macrophages with phagocytosed MWCNT are capable of inducing granuloma which in turn restricts the mobility of the nanotubes, thus increasing the biopersistence. Similar histopathological findings reported by several other workers [9,18,25,33] showed that the inhalation of MWCNTs induces mono and polymorphonuclear inflammatory cell infiltration, impairment of function of alveolar macrophages, epithelial cell hyperplasia, peribronchiolar inflammation and microgranulomas in lungs. These reports support our present findings.

## 4. Conclusion

We have investigated the effect of single exposure of MWCNT in rats by intermittent sacrifice. The effects were monitored by BALF and histopathological analysis. We interpret that MWCNT induces inflammation, fibrosis and granuloma characterized by progressive elevation of TNF alpha and IL-4. Histopathological studies further support our view and reveal the distribution of MWCNT in lungs and TBLN. We conclude that MWCNT-induced pulmonary toxicity is considerable even on single exposure. As the occupational and intentional exposure to MWCNT is increasing now-a-days, we warrant the urgent need to explore its repeated dose toxicity and validate an appropriate antitoxic candidate.

## Conflict of interest

The authors declare that there are no conflicts of interest

## Transparency document

The Transparency document associated with this article can be found in the online version.

## Acknowledgements

The authors APF and TD would like to acknowledge DRDO, New Delhi for providing financial assistance to carry out the project (No: ERIP/ER/1103944/M/01/1359).

## References

[1] C.R. Martin, P. Kohli, The emerging field of nanotube biotechnology, Nat. Rev. Drug. Discov. 2 (2003) 29–37.
[2] M.F.L. De Volder, S.H. Tawfick, R.H. Baughman, A.J. Hart, Carbon nanotubes: present and future commercial applications, Science 339 (2013) 535–539.

[3] A.D. Maynard, P.A. Baron, M. Foley, A.A. Shvedova, E.R. Kisin, V. Castranova, Exposure to carbon nanotube material: aerosol release during the handling of unrefined single-walled carbon nanotube material, J. Toxicol. Environ. Health A 67 (2004) 87–107.
[4] C.W. Lam, J.T. James, R. McCluskey, R.L. Hunter, Pulmonary toxicity of single-wall carbon nanotubes in mice 7 and 90 days after intratracheal instillation, Toxicol. Sci. 77 (2004) 126–134.
[5] A.A. Shvedova, E.R. Kisin, R. Mercer, A.R. Murray, V.J. Johnson, A.I. Potapovich, Y.Y. Tyurina, O. Gorelik, S. Arepalli, D. Schwegler-Berry, A.F. Hubbs, J. Antonini, D.E. Evans, B.K. Ku, D. Ramsey, A. Maynard, V.E. Kagan, V. Castranova, P. Baron, Unusual inflammatory and fibrogenic pulmonary responses to single walled carbon nanotubes in mice, Am. J. Physiol. Lung Cell Mol. Physiol. 289 (2005) L698–L708.
[6] J.G. Li, W.X. Li, J.Y. Xu, X.Q. Cai, R.L. Liu, Y.L. Li, Q.F. Zhao, Q.N. Li, Comparative study of pathological lesions induced by multiwalled carbon nanotubes in lungs of mice by intratracheal instillation and inhalation, Environ. Toxicol. 22 (2007) 415–421.
[7] Y. Morimoto, M. Hirohashi, M. Horie, A. Ogami, T. Oyabu, T. Myojo, M. Hashiba, Y. Mizuguchi, T. Kambara, B.W. Lee, E. Kuroda, M. Shimada, W.N. Wang, K. Mizuno, K. Yamamoto, K. Fujita, J. Nakanishi, I. Tanaka, Pulmonary toxicity of well-dispersed single-wall carbon nanotubes following intratracheal instillation, J. Nano Res. 18–19 (2012) 9–25.
[8] C.A. Poland, R. Duffin, I. Kinloch, A. Maynard, W.A. Wallace, A. Seaton, V. Stone, S. Brown, W. Mac-Nee, K. Donaldson, Carbon nanotubes introduced into the abdominal cavity of mice show asbestos-like pathogenicity in a pilot study, Nat. Nanotechnol. 3 (2008) 423–428.
[9] L. Ma-Hock, S. Treumann, V. Strauss, S. Brill, F. Luizi, M. Mertler, K. Wiench, A.O. Gamer, B. Van Ravenzwaay, R. Landsiedel, Inhalation toxicity of multiwall carbon nanotubes in rats exposed for 3 months, Toxicol. Sci. 112 (2009) 468–481.
[10] J. Pauluhn, Subchronic 13-week inhalation exposure of rats to multiwalled carbon nanotubes: toxic effects are determined by density of agglomerate structures, not fibrillar structures, Toxicol. Sci. 113 (2010) 226–242.
[11] J.P. Ryman-Rasmussen, E.W. Tewksbury, O.R. Moss, M.F. Cesta, B.A. Wong, J.C. Bonner, Inhaled multiwalled carbon nanotubes potentiate airway fibrosis in murine allergic asthma, Am. J. Respir. Cell Mol. Biol. 40 (2009) 349–358.
[12] T. Myojo, A. Ogami, T. Oyabu, Y. Morimoto, M. Hirohashi, M. Murakami, K. Nishi, C. Kadoya, I. Tanaka, Risk assessment of airborne fine particles and nanoparticles, Adv. Powder Technol. 21 (2010) 507–512.
[13] L. Geraets, A.G. Oomen, J.D. Schroeter, V.A. Coleman, F.R. Cassee, Tissue distribution of inhaled micro- and nano-sized cerium oxide particles in rats: results from a 28-day exposure study, Toxicol. Sci. 127 (2012) 463–473.
[14] A. Srinivas, P. Jaganmohan Rao, G. Selvam, P. Balakrishna Murthy, P. Neelakanta Reddy, Acute inhalation toxicity of cerium oxide nanoparticles in rats, Toxicol. Lett. 205 (2011) 105–115.
[15] G. Oberdorster, J.N. Finkelstein, C. Johnston, R. Gelein, C. Cox, R. Baggs, A.C. Elder, Acute pulmonary effects of ultrafine particles in rats and mice, Res. Rep. Health Eff. Inst. 96 (2000) 5–74.
[16] J.H. Ji, J.H. Jung, S.S. Kim, J.U. Yoon, J.D. Park, B.S. Choi, Y.H. Chung, I.H. Kwon, J. Jeong, B.S. Han, J.H. Shin, J.H. Sung, K.S. Song, I.J. Yu, Twenty eight day inhalation toxicity study of silver nanoparticles in Sprague–Dawley rats, Inhal. Toxicol. 19 (2007) 857–871.
[17] D.B. Warheit, T.R. Webb, V.L. Colvin, K.L. Reed, C.M. Sayes, Pulmonary bioassay studies with nanoscale and fine-quartz particles in rats: toxicity is not dependent upon particle size but on surface characteristics, Toxicol. Sci. 95 (2007) 270–280.
[18] Y. Umeda, T. Kasai, M. Saito, H. Kondo, T. Toya, S. Aiso, H. Okuda, T. Nishizawa, S. Fukushima, Two-week toxicity of multi-walled carbon nanotubes by whole body inhalation exposure in rats, J. Toxicol. Pathol. 26 (2013) 131–140.
[19] M. Drent, N.A.M. Cobben, R.F. Henderson, E.F.M. Wouters, M. Van Dieijen-Visser, Usefulness of lactate dehydrogenase and its isoenzymes as indicators of lung damage or inflammation, Eur. Respir. J. 9 (1996) 1736–1742.
[20] M. Van Krugten, N.A. Cobben, R.J. Lamers, M.P. Van Dieijen-Visser, S.S. Wagenaar, E.F. Wouters, M. Drent, Serum LDH: a marker of disease activity and its response to therapy in idiopathic pulmonary fibrosis, Neth. J. Med. 48 (1996) 220–223.
[21] M.F. Cesta, J.P. Ryman-Rasmussen, D.G. Wallace, T. Masinde, G. Hurlburt, A.J. Taylor, J.C. Bonner, Bacterial lipopolysaccharide enhances PDGF signaling and pulmonary fibrosis in rats exposed to carbon nanotubes, Am. J. Respir. Cell Mol. Biol. 43 (2010) 142–151.
[22] N. Kobayashi, M. Naya, E. Makoto, S. Endoh, J. Maru, K. Mizuno, J. Nakanishi, Biological response and morphological assessment of individually dispersed multi-wall carbon nanotubes in the lung after intratracheal instillation in rats, Toxicology 276 (2010) 143–153.
[23] R.F. Henderson, G.G. Scott, J.J. Waide, Source of alkaline phosphatase activity in epithelial lining fluid of normal and injured F344 rat lungs, Toxicol. Appl. Pharmacol. 134 (1995) 170–174.
[24] A. Capelli, M. Lusuardi, C.G. Cerutti, C.F. Donner, Lung alkaline phosphatase as a marker of fibrosis in chronic interstitial disorders, Am. J. Respir. Crit. Care Med. 155 (1997) 249–253.
[25] L. Ma-Hock, V. Strauss, S. Treumann, K. Küttler, W. Wohlleben, T. Hofmann, S. Gröters, K. Wiench, B. van Ravenzwaay, R. Landsiedel, Comparative inhalation toxicity of multi-wall carbon nanotubes, graphene, graphite nanoplatelets and low surface carbon black, Part. Fibre Toxicol. 10 (2013) 23.
[26] A.A. Shvedova, E. Kisin, A.R. Murray, V.J. Johnson, O. Gorelik, S. Arepalli, A.F. Hubbs, R.R. Mercer, P. Keohavong, N. Sussman, J. Jin, J. Yin, S. Stone, B.T. Chen, G. Deye, A. Maynard, V. Castranova, P.A. Baron, V.E. Kagan, Inhalation vs. aspiration of single-walled carbon nanotubes in C57BL/6 mice: inflammation, fibrosis, oxidative stress, and mutagenesis, Am. J. Physiol. Lung Cell Mol. Physiol. 295 (2008) L552–L565.
[27] D.M. Brown, I.A. Kinloch, U. Bangert, A.H. Windle, D.M. Walter, G.S. Walker, C.A. Scotchford, K. Donaldson, V. Stone, An in vitro study of the potential of carbon nanotubes and nanofibres to induce inflammatory mediators and frustrated phagocytosis, Carbon 45 (2007) 1743–1756.
[28] E.J. Park, W.S. Cho, J. Jeong, J.H. Yi, K. Choi, Y. Kim, K. Park, Induction of inflammatory responses in mice treated with cerium oxide nanoparticles by intratracheal instillation, J. Health Sci. 56 (2010) 387–396.
[29] Y. Morimoto, M. Hirohashi, A. Ogami, T. Oyabu, T. Myojo, M. Todoroki, M. Yamamoto, M. Hashiba, Y. Mizuguchi, B.W. Lee, E. Kuroda, M. Shimada, W.N. Wang, K. Yamamoto, K. Fujita, S. Endoh, K. Uchida, N. Kobayashi, K. Mizuno, M. Inada, H. Tao, T. Nakazato, J. Nakanishi, I. Tanaka, Pulmonary toxicity of well-dispersed multi-wall carbon nanotubes following inhalation and intratracheal instillation, Nanotoxicology 6 (2012) 587–599.
[30] R. Eferl, P. Hasselblatt, M. Rath, H. Popper, R. Zenz, V. Komnenovic, M.H. Idarraga, L. Kenner, E.F. Wagner, Development of pulmonary fibrosis through a pathway involving the transcription factor Fra-2/AP-1, PNAS 105 (2008) 10525–10530.
[31] F. Huaux, T. Liu, B. McGarry, M. Ullenbruch, S.H. Phan, Dual roles of IL-4 in lung injury and fibrosis, J. Immunol. 170 (2003) 2083–2092.
[32] J. Muller, F. Huaux, N. Moreau, P. Misson, J.F. Heilier, M. Delos, M. Arras, A. Fonseca, J.B. Nagy, D. Lison, Respiratory toxicity of multi-wall carbon nanotubes, Toxicol. Appl. Pharm. 207 (2005) 221–231.
[33] A. Erdely, M. Dahm, B.T. Chen, P.C. Zeidler-Erdely, J.E. Fernback, M.E. Birch, D.E. Evans, M.L. Kashon, J.A. Deddens, T. Hulderman, S.A. Bilgesu, L. Battelli, D. Schwegler-Berry, H.D. Leonard, W. McKinney, D.G. Frazer, J.M. Antonini, D.W. Porter, V. Castranova, M.K. Schubauer-Berigan, Carbon nanotube dosimetry: from workplace exposure assessment to inhalation toxicology, Part. Fibre Toxicol. 10 (2013) 53.
[34] National Institute for Occupational Safety and Health, NIOSH Pocket Guide to Chemical Hazards – Graphite (synthetic), Centers for Disease Control and Prevention, 2010 http://www.cdc.gov/niosh/npg/